

Single cell cloning generates lung endothelial colonies with conserved growth, angiogenic, and bioenergetic characteristics

Ji Young Lee^{1,2,3,4}, Sarah A. McMurtry^{1,4} and Troy Stevens^{1,2,4}

¹Department of Physiology and Cell Biology, University of South Alabama, Mobile, AL, USA; ²Department of Internal Medicine, University of South Alabama, Mobile, AL, USA; ³Division of Pulmonary and Critical Care Medicine, University of South Alabama, Mobile, AL, USA; ⁴Center for Lung Biology, University of South Alabama, Mobile, AL, USA

Abstract

Pulmonary artery, capillary, and vein endothelial cells possess distinctive structures and functions, which represent a form of vascular segment specific macroheterogeneity. However, within each of these segmental populations, individual cell functional variability represents a poorly characterized microheterogeneity. Here, we hypothesized that single cell clonogenic assays would reveal microheterogeneity among the parent cell population and enable isolation of highly representative cells with committed parental characteristics. To test this hypothesis, pulmonary microvascular endothelial cells (PMVECs) and pulmonary arterial endothelial cells (PAECs) were isolated from different Sprague Dawley rats. Serum stimulated proliferation of endothelial populations and single cell clonogenic potential were evaluated. In vitro Matrigel assays were utilized to analyze angiogenic potential and the Seahorse assay was used to evaluate bioenergetic profiles. PMVEC populations grew faster and had a higher proliferative potential than PAEC populations. Fewer PMVECs were needed to form networks on Matrigel when compared with PAECs. PMVECs primarily utilized aerobic glycolysis, while PAECs relied more heavily on oxidative phosphorylation, to support bioenergetic demands. Repeated single cell cloning and expansion of PAEC colonies generated homogeneous first-generation clones that were highly reflective of the parental population in terms of growth, angiogenic potential, and bioenergetic profiles. Repeated single cell cloning of the first-generation clones generated second-generation clones with increased proliferative potential while maintaining other parental characteristics. Second-generation clones were highly homogeneous populations. Thus, single cell cloning reveals microheterogeneity among the parent cell population and enables isolation of highly representative cells with parental characteristics.

Keywords

pulmonary circulation, heterogeneity, metabolism, proliferation, aerobic glycolysis

Date received: 2 April 2017; accepted: 3 August 2017

Pulmonary Circulation 2017; 7(4) 777–792

DOI: 10.1177/2045893217731295

Introduction

Pulmonary endothelium is structurally and functionally heterogeneous along the artery-to-capillary-to-vein axis.¹ This macroheterogeneity among endothelial phenotypes can be resolved in vivo using anatomical determinants, including the differential expression of junctional and matrix proteins and the distribution of various organelles, such as Weibel-Palade bodies that are most prominently seen in endothelium within conduit or large vessel segments.^{2–4} Lectin binding has also contributed to identification of endothelial macroheterogeneity, where

Griffonia simplicifolia recognizes microvascular but not extra-alveolar endothelium.^{5–7} Lectin binding selectivity has enabled investigators to isolate and subculture endothelial cells that retain characteristics of their in vivo function. For example, *Griffonia simplicifolia*-positive pulmonary microvascular endothelial cells (PMVECs) are

Corresponding author:

Troy Stevens, Department of Physiology and Cell Biology, Center for Lung Biology College of Medicine, University of South Alabama, Mobile, AL 36688, USA.

Email: tstevens@southalabama.edu



Creative Commons Non Commercial CC-BY-NC: This article is distributed under the terms of the Creative Commons Attribution-NonCommercial 4.0 License (<http://www.creativecommons.org/licenses/by-nc/4.0/>)

which permits non-commercial use, reproduction and distribution of the work without further permission provided the original work is attributed as specified on the SAGE and Open Access pages (<https://us.sagepub.com/en-us/nam/open-access-at-sage>).

© The Author(s) 2017.

Reprints and permissions:
sagepub.co.uk/journalsPermissions.nav
journals.sagepub.com/home/pul



pro-proliferative and angiogenic when compared to their macrovascular counterparts.⁸ The microvascular endothelial cells also possess a more restrictive barrier to macromolecules and they are less sensitive to barrier disruption induced by neurohumoral inflammatory mediators, when compared with pulmonary artery and vein endothelial cells.^{9–11} In contrast, PMVECs are more sensitive to barrier disruption induced by neuraminidase(s).¹² Interestingly, these subcultured cells retain a memory of their origin, even when they are reintroduced into the pulmonary circulation.¹³ Pulmonary artery endothelial cell (PAEC) infusion into an acellular lung scaffold results in repopulation of the artery and not the capillary or vein segments. In contrast, pulmonary vein endothelial cell infusion in this model results in repopulation of vein and not the arterial or capillary segments, and PMVECs are the only phenotype that repopulates capillaries. Thus, an important, stable macroheterogeneity is apparent among endothelial cells derived from artery, capillary, and vein segments.

Evidence for endothelial macroheterogeneity among vascular segments provides important insight into the integrated function of arteries, capillaries, and veins, and it also contributes to our understanding of how vascular disease manifests in discrete vascular locations.^{14–17} However, this large-scale heterogeneity does not inform us as to how endothelium interprets and responds to the complexity of chemical and biophysical inputs that are present within a discrete vascular segment. Studies on the endothelial response to inflammation illustrate that whereas neurohumoral inflammatory mediators induce interendothelial cell gaps, e.g. breach junctional integrity, two adjacent cells do not respond uniformly to the same stimulus.¹⁸ These inflammatory mediators and other vasoregulatory autocooids do not induce identical intracellular signals in adjacent cells. Such a subcellular heterogeneity has been regularly reported in studies of cytosolic calcium, especially as work has moved from measurements of global cytosolic calcium to more refined studies on dynamic calcium transients, where dynamic complexity in, and the spatial constraints of, cytosolic calcium encodes unique cellular information.^{19,20} So, while endothelium within a vascular segment is self-similar, especially when compared to endothelium from a different vascular site, there is clear microheterogeneity that remains incompletely explored.

The relevance of cellular microheterogeneity as a determinant of endothelial growth, e.g. vessel renewal, has been considered. Schwartz and Benditt mapped constitutive thymidine incorporation in an aortic vessel wall and determined that the daily rate of endothelial replication approximates 50%.²¹ However, the distribution of replicating cells was not uniform, but rather, localized to apparent niches within the vessel wall. Evidence that some vascular niches are highly proliferative whereas others are not is consistent with the idea that replication competent cells represent progenitors that reconstitute an entire hierarchy of growth potentials. Yoder utilized single cell clonal analysis to reveal niches of

replication competent endothelial cells residing within a larger colony of cells.^{22–24} In subcultures of both circulating and tissue resident endothelial cells, Yoder et al. found a hierarchy of growth potentials among single cells, where individual cells give rise to colonies of low, intermediate, and high replication competence. Single cell sorting of the high proliferative potential colonies fully recapitulates the growth hierarchy of low, intermediate, and high replication competent progeny, suggesting high proliferative potential cells are progenitor in nature. These highly proliferative cells are also rapidly angiogenic, leading to the idea that within a vessel wall, niches of cells are diverse, where some are epigenetically encoded to renew the endothelium and others are not.²⁴

Mapping the distribution of progenitor cell niches in vivo has presented a challenge, especially in pulmonary circulation. Sims-Lucas et al. recently identified a population of FoxD1 positive progenitor cells within the lung and kidney mesenchyme that give rise to angiogenic endothelium during development, consistent with the idea that replication competent progenitor niches are embedded within the lung microcirculation.²⁵ Subcultures of PMVECs also display a hierarchy of single cell growth potentials that is characteristic of a progenitor niche,²⁶ similar to the work of Yoder et al.^{22–24} Single cell cloning of PMVECs and PAECs demonstrates an abundance of highly proliferative single cells within the microvascular endothelial cell culture. These cells utilize aerobic glycolysis to maintain rapid growth and neo-angiogenesis.⁸ In contrast, PAECs grow slowly, possess a low abundance of highly proliferative potential cells within the colony, and are less angiogenic. Nonetheless, expansion of the relatively few highly proliferative potential PAECs yields a rapidly growing subpopulation that, despite their rapid growth, retains commitment to the parental endothelial cell lineage. It remains unclear whether single cell clones isolated from these fast-growing PAECs faithfully recapitulate the behavior of their parent cells. Here, we provide evidence that single cell clones from highly proliferative potential PAECs grow into homogeneous cell populations with conserved growth, angiogenic, and bioenergetic functions.

Materials and methods

Isolation of rat lung endothelial cells. Procedures for isolation of rat endothelial cells were approved by the University of South Alabama Institutional Animal Care and Use Committee. PMVECs and PAECs were isolated from male Sprague Dawley rats as previously described.^{27,28} Whereas PMVECs are isolated from vessels $\leq 25 \mu\text{m}$ in diameter, mostly reflective of capillaries, PAECs are isolated from the main pulmonary artery and two to three additional vessel branches.^{6,14,16,17} For the purposes of this study, cells were isolated from four different Sprague Dawley rats. PMVECs were isolated from two different rats and PAECs were isolated from two additional rats.

Growth curves. On day 0, cells were seeded at a density of 10^5 cells per well in six-well plates in DMEM (4.5 g/L glucose), 10% FBS, and 1% penicillin-streptomycin, and grown for seven days (days 1–7) without media change at 37°C in room air, 5% CO₂. Cells were photographed, trypsinized, and counted using a Coulter Counter (Beckman Coulter, Hialeah, FL, USA) every 24 h.

Single cell cloning. Single cell clonogenic assays were performed as described elsewhere.^{22,24,26,29} Cells were trypsinized, transferred to flow cytometry tubes containing standard culture media at 5×10^5 cells/tubes. Cells were typically seeded at single cell density on four 96-well plates containing 200 µL/well of DMEM (4.5 g/L glucose), 10% FBS, and 1% penicillin-streptomycin using a FACS sorter. Cells were cultured at 37°C with 5% CO₂-room air for 14 days without media change. On day 14, each well was examined by light microscopy to assess colony size and representative wells were photographed.

Isolation of single cell colonies. Colonies were randomly selected from 96-well plates and expanded by trypsinizing and seeding to dishes of progressively larger growth area using standard culture media and technique.

Matrigel network formation assay. Matrigel (356231, Corning) was thawed overnight at 4°C. On the day of the experiment, Matrigel was loaded (30 µL per well) in 96-well plates while the plates are kept on top of ice. The plates were incubated at 37°C with 5% CO₂-room air for 1 h. Cells were trypsinized from 10-cm dishes when approximately 70% confluent and seeded at cell type specific optimal densities ($4.0\text{--}8.0 \times 10^4$ cells per well), with a total cell solution volume of 80 µL per well. Cells were incubated at 37°C with 5% CO₂-room air for 24 h. Pictures were taken at 24 h. Images were analyzed using the “Angiogenesis Analyzer” tool, programmed in ImageJ’s macro language.

Metabolic assay. Mitochondrial and glycolysis stress tests were conducted using the Seahorse extracellular flux analyzer (Seahorse XF24 analyzer, Seahorse Bioscience, MA, USA). A cartridge was loaded with calibration solution and kept overnight at 37°C according to the manufacturer’s protocol. On the day of the experiment, cells were seeded in 24-well plates (40,000 cells per well) in DMEM (4.5 g/L glucose), 10% FBS, and 1% penicillin-streptomycin and kept at 37°C in an incubator with 5% CO₂. Four hours later, cells were washed with serum-free XF Seahorse Base media supplemented with GlutaMAX 2 mM, sodium pyruvate 1 mM, and glucose of different concentrations, 25 or 0 mM for mitochondrial and glycolysis stress tests, respectively. Using the analyzer, oxygen consumption rate (OCR) and extracellular acidification rate (ECAR) were evaluated over time (0–69 min). For the mitochondrial stress test, cells were challenged with four different mitochondrial stressors, including oligomycin, carbonyl cyanide-4-(trifluoromethoxy) phenylhydrazone (FCCP), antimycin A, and rotenone 1 µM final concentration for each. For the glycolysis stress test, cells were challenged with three reagents,

including glucose 10 mM, oligomycin 1 µM, and 2-deoxyglucose (2-DG) 100 mM final concentrations.

Reagents. DMEM (4.5 g/L D-glucose, L-glutamine, 11965-092 Gibco by Life Technologies), sodium pyruvate (S8636, Sigma), GlutaMAX™-I (35050-061, Gibco by Life Technologies), oligomycin from *Streptomyces diastatochromogenes* (O4876, Sigma), carbonyl cyanide 4-(trifluoromethoxy)phenylhydrazone (CCCP, Sigma, C2920), antimycin A (A8674, Sigma), rotenone (R8875, Sigma), D-(+)-Glucose (G8270, Sigma), 2-deoxy-D-glucose (D6134, Sigma), and dimethyl sulfoxide (DMSO, D8418, Sigma).

Statistics. One- and two-way ANOVA and Student’s *t*-tests were used for statistical analyses, as appropriate. Bonferroni post hoc was used, as appropriate. Significance was denoted as $P < 0.05$.

Results

PMVECs grow faster and have a higher proliferative potential than PAECs. Previously, we have demonstrated that PMVEC populations grow faster⁸ and have a higher percentage of highly proliferative potential cells²⁶ than PAEC populations. To confirm our previous findings, we repeated growth curves and single cell clonogenic assays on pulmonary endothelial cells from four different Sprague-Dawley rats; PMVEC 1, PMVEC 2, PAEC 1, and PAEC 2. Consistent with our previous findings, PMVECs grew faster than PAECs in population, as evidenced by a faster doubling time (PMVECs = 33.6, PAECs = 50.7) (Fig. 1a). PMVECs grew from 10^5 to 1.5×10^6 cells in one week whereas PAECs grew from 10^5 to 1.0×10^6 cells over this time course ($P < 0.05$). PMVECs induced an acidic color change of phenol red containing medium, consistent with the idea that they utilize aerobic glycolysis to sustain the ATP demands of proliferation. PAECs did not rely on aerobic glycolysis to sustain their growth.

We then performed single cell clonogenic assays, where cells are seeded at a single cell density and grown for 14 days. PMVECs grew in medium- (500–2000 cells) to large- (> 2000 cells) sized colonies, and all of these medium- to large-sized colonies acidified the medium. On the other hand, PAECs either formed small colonies (PMVECs vs. PAECs, 55% vs. 100%, $P < 0.05$) or did not divide (Fig. 1b). These data support the idea that PMVECs grow faster than PAECs do in population, due to a higher percentage of replication competent cells.

PMVECs and PAECs form networks on Matrigel. Angiogenic capacity is an important characteristic of endothelial cells. Our previous work has suggested that PMVECs are rapidly angiogenic when compared to PAECs. We conducted in vitro Matrigel assays, which enable assessment of network formation. PMVECs and PAECs were initially seeded at different densities, $4.0 \times 10^4\text{--}1.6 \times 10^5$ cells per well, to determine an optimal number of cells required for stable network formation. Both PMVEC 1 and 2 formed

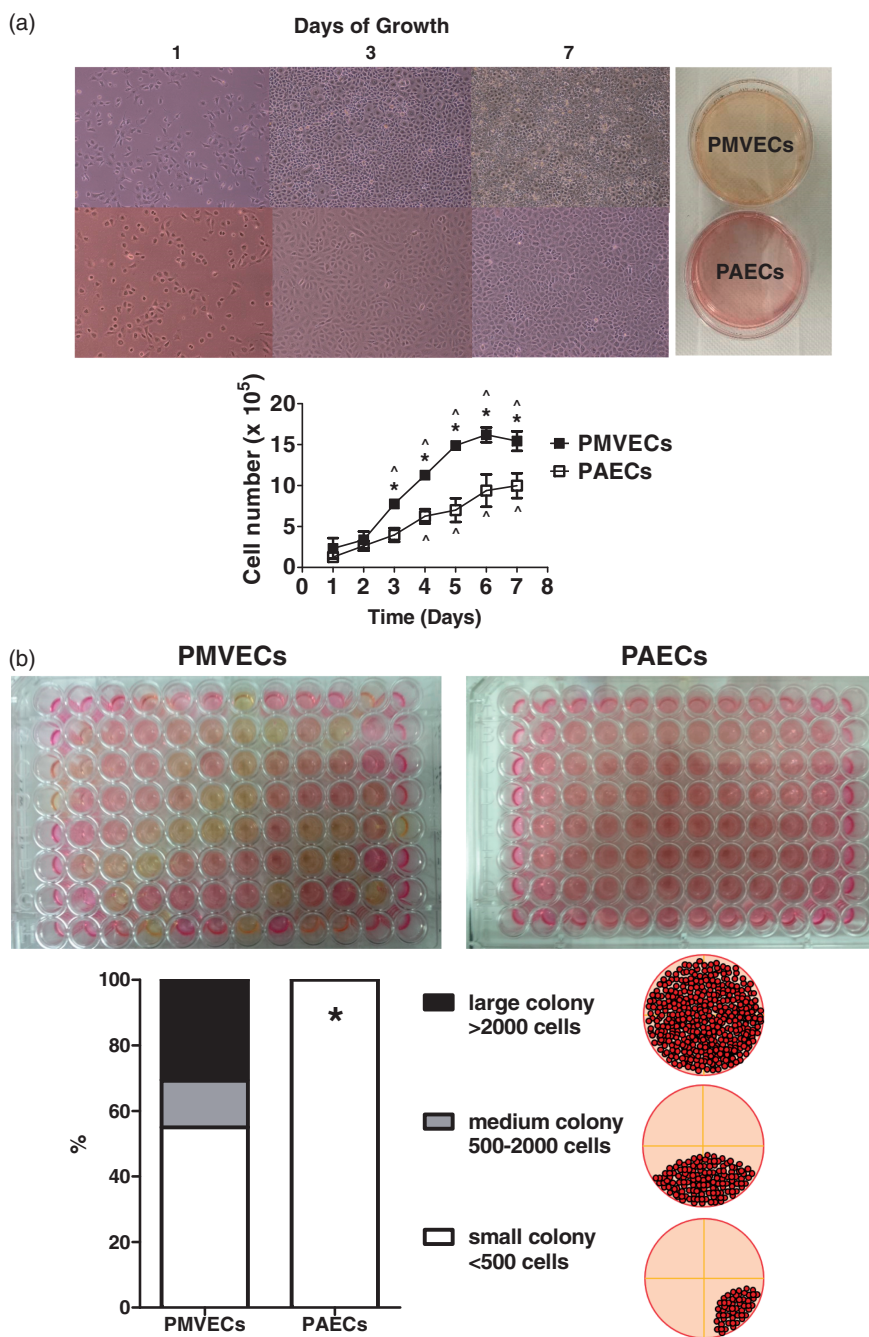


Fig. 1. PMVECs grow faster, have a high proliferative potential, and have a propensity to form networks. (a) Serum stimulated growth of PMVECs and PAECs were assessed for seven days. PMVECs grew faster than PAECs. Data represent mean \pm standard deviation. One-way ANOVA was used to assess significance over the seven-day time course and two-way ANOVA and Bonferroni post hoc tests were used to compare between cell types. For each cell type, two separate experiments were performed using a total of four wells. * denotes significantly different ($P < 0.05$) in PMVECs vs. PAECs (n = number of different cell types, 2 and 4 for PMVECs and PAECs, respectively). ^ denotes significantly different ($P < 0.05$) from baseline at day 1. (b) PMVECs and PAECs were seeded one cell per well on 96-well plates, four plates per cell type, by FACS sorter. Plates were examined on day 14. PMVECs had a higher percentage of medium and large colonies than PAECs. Data represent the average of percent colony counts for each colony size. Student's t -test was used to compare the percentages of different colony sizes between PMVECs and PAECs. *denotes significant difference ($P < 0.05$) in small colony counts (<500 cells) between PMVECs and PAECs groups (n = 2 and 4, respectively). (c, d) PMVECs and PAECs were seeded on Matrigel coated 96-well plates at 4.0×10^4 and 8.0×10^4 cells per well, respectively. Images were obtained 24 h after seeding at $10 \times$ magnification. (c) Representative images are shown for each cell type. (d) Networks were quantified by ImageJ software. PMVECs formed networks with relatively thin webs and larger luminal areas compared to PAECs. Data represent mean \pm standard deviation. Images from three independent experiments were used for each group. Student's t -test was used to compare two cell types. *denotes significant difference ($P < 0.05$).

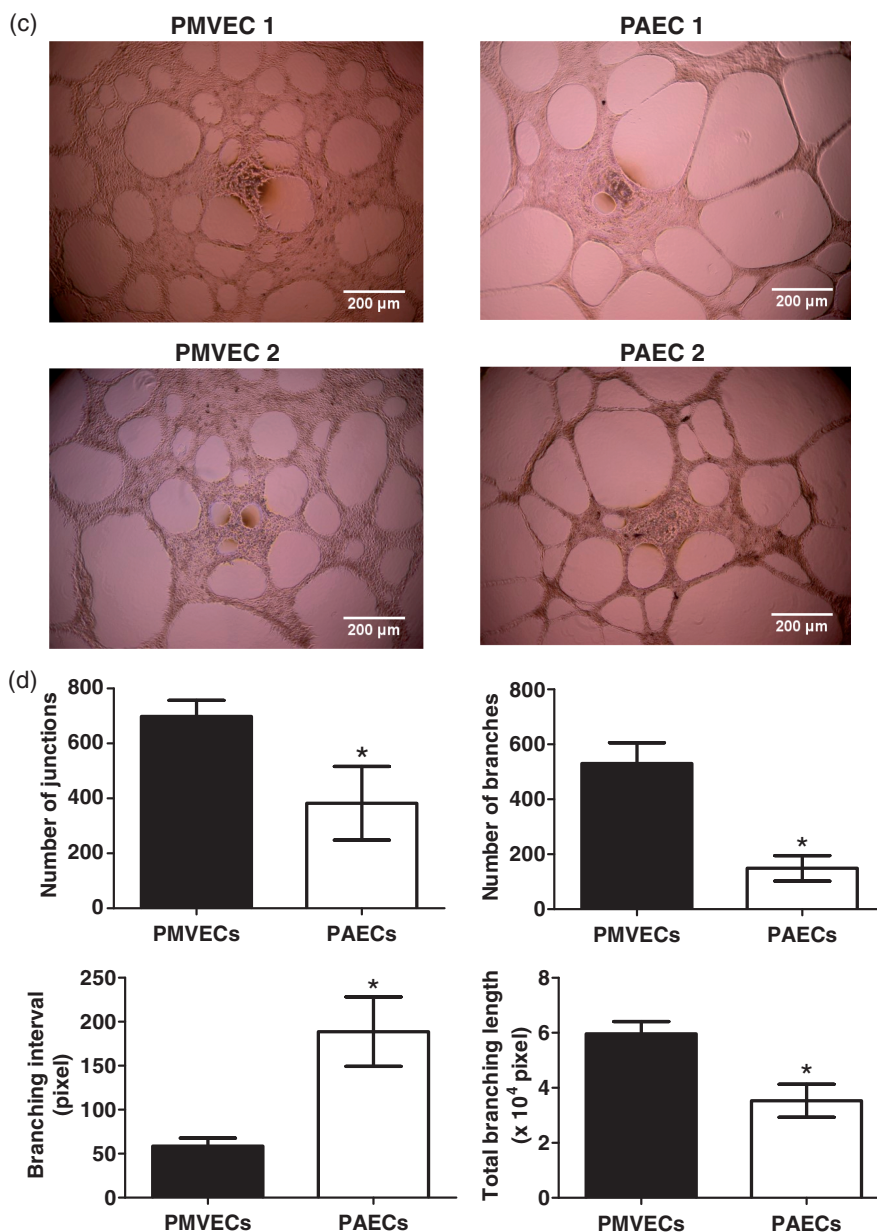


Fig. 1. Continued.

stable (lasting at least 24 h) networks when cells were seeded at 4.0×10^4 cells per well (Fig. 1c). However, PAEC 1 and 2 required twice as many cells, 8.0×10^4 cells per well, to make equivalently stable networks. When a higher or lower number of PAECs were loaded into Matrigel, the cells either did not form closed networks or they collapsed prematurely before 24 h. Network quantification by ImageJ showed lower numbers of junctions and branches, higher branching intervals and a lower total branching length (Fig. 1d). These findings suggest that PAECs form denser networks and it supports the notion that PMVECs support rapid neo-angiogenesis. Whether this characteristic is applicable in vivo and whether it plays any role in angiogenesis of different vessel size is unclear.

Whereas PMVECs utilize aerobic glycolysis, PAECs are more reliant on oxidative phosphorylation. We have previously demonstrated that PMVECs have higher glucose consumption, proton and lactate generation, and lower oxygen consumption than PAECs, collectively suggesting PMVECs and PAECs sustain ATP demands through distinct bioenergetic pathways.⁸ To determine whether our earlier findings are generalizable to cells from different individual rats, we assessed metabolic profiles of cells from four distinct rats. To confirm the specificity of metabolic parameters in relation to oxidative phosphorylation or aerobic glycolysis, we performed mitochondrial and glycolysis stress tests using the Seahorse extracellular flux analyzer. In this assay, OCR and ECAR are monitored over time as surrogate markers for the

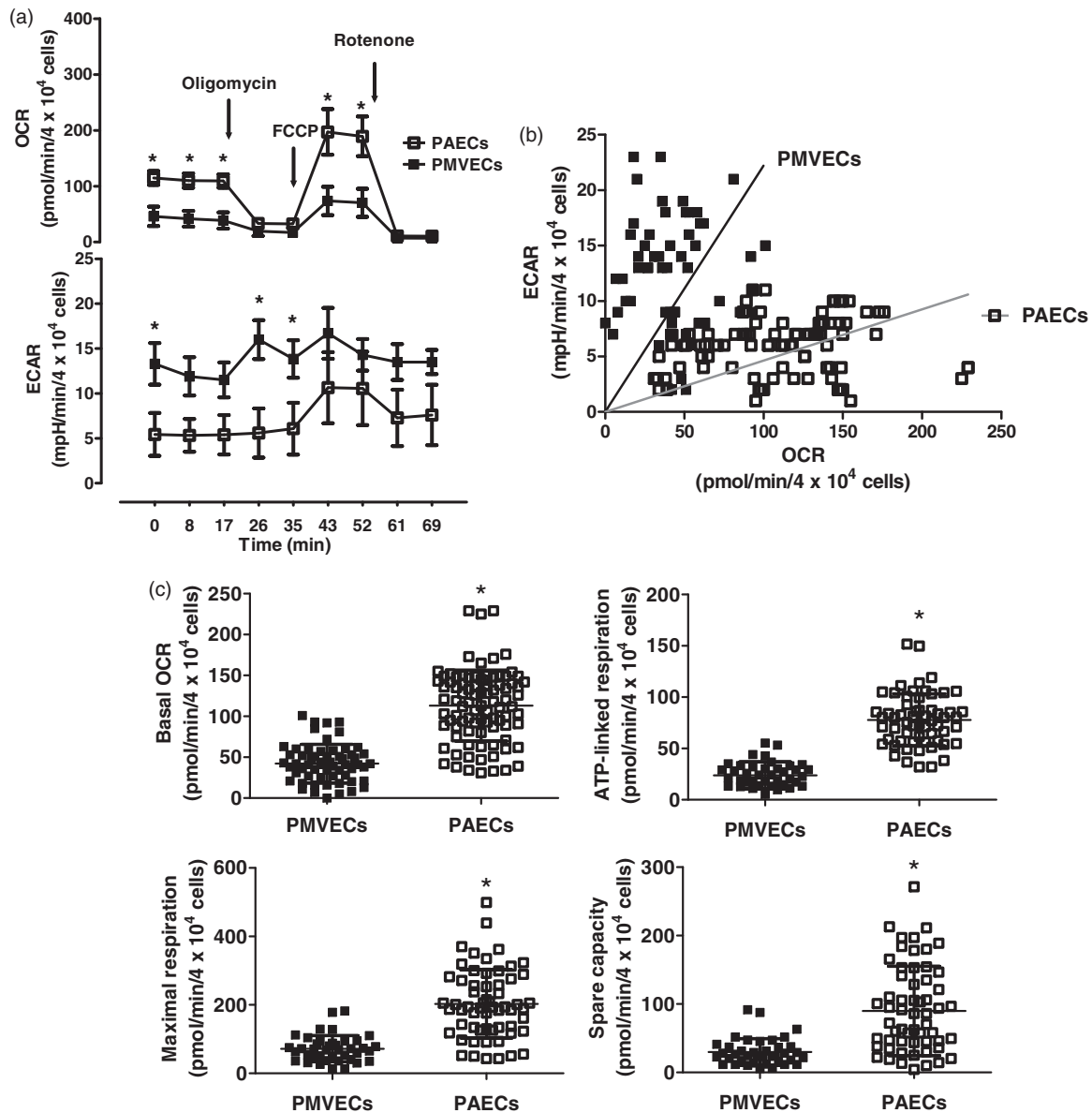


Fig. 2. Whereas PMVECs utilize aerobic glycolysis, PAECs are more reliant on oxidative phosphorylation, to meet metabolic demands. (a–e) PMVECs and PAECs were grown to confluence in 100-mm dishes and the principal bioenergetic pathways were determined by mitochondrial (a–c) and glycolysis (d) stress tests, using the Seahorse extracellular flux analyzer. (a, d) OCR and ECAR at baseline and with mitochondrial (oligomycin, FCCP, and rotenone) and glycolytic (glucose, oligomycin, and 2-DG) stressors are shown over time. PMVECs utilize aerobic glycolysis whereas PAECs utilize oxidative phosphorylation as their primary metabolic pathway. Data represent mean \pm standard error. Two-way ANOVA and Bonferroni post hoc test were used to compare between cell types. Results from five independent experiments, each with five replicates, a total of 20–30 wells per group are shown. *denotes significantly different ($P < 0.05$) in PMVECs vs. PAECs ($n = 4$ –5 per group). (b) OCR and ECAR at baseline of mitochondrial stress test at three different time points are depicted. Each dot represents the value of each individual well. (c) Basal OCR, ATP-linked respiration (average basal OCR – oligomycin response), maximal respiration (FCCP response) and spare capacity (maximal OCR – average basal OCR) are noted. (e) OCR at baseline of glycolysis stress test at three different time points are depicted. Each dot represents the value of individual well. Student's t -test was used. *denotes significant difference ($P < 0.05$) between PMVECs and PAECs groups. Each dot represents the value of individual well at each time point.

degree of oxidative phosphorylation and aerobic glycolysis utilization, respectively.

In mitochondrial stress tests, where we included 25 mM of glucose in the assay medium throughout the experiment as a substrate for glycolysis, PMVECs showed lower OCR

(PMVECs vs. PAECs, $P < 0.05$) and higher ECAR (PMVECs vs. PAECs, $P < 0.05$) at baseline when compared with PAECs (Fig. 2a, b). Responses to different mitochondrial stressors, including oligomycin, FCCP, and rotenone, confirmed that higher OCR of PAECs is from increased

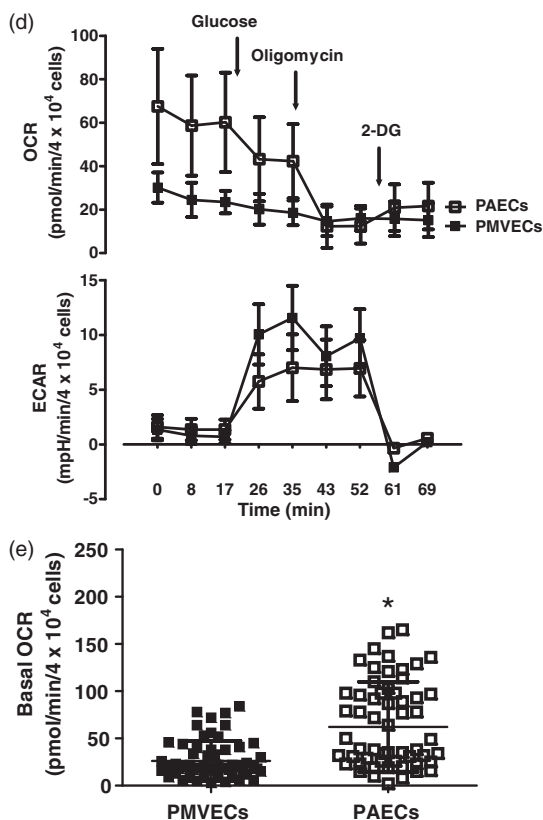


Fig. 2. Continued.

utilization of mitochondrial oxidative phosphorylation. Additional parameters for mitochondrial function, basal OCR, ATP-linked respiration, maximal respiration and spare capacity, were all lower in PMVECs compared with PAECs (Fig. 2c).

In glycolysis stress tests, where the assay media was glucose free, there was no difference in baseline ECAR between PMVECs and PAECs (PMVECs vs. PAECs, $P = ns$), while OCR was higher in PAECs (PMVECs vs. PAECs, $P < 0.05$) (Fig. 2d, e). These results suggest that PMVECs have suppressed aerobic glycolysis due to the absence of glucose as a primary substrate at baseline. Upon glucose challenge, ECAR was significantly increased to a higher degree in PMVECs, which was again suppressed by 2-DG, an ineffective substrate for glycolysis. Both groups had little glycolytic reserve, which is represented by the difference between glucose induced and oligomycin induced ECAR changes. Thus, both cell types tend to maximally utilize glycolysis when the substrate is abundant, although PMVECs are most reliant upon aerobic glycolysis.

Single cell cloning generates homogeneous first-generation clones reflective of the parent population. We identified the hierarchy of growth potentials by single cell clonogenic assays (Fig. 1b). Unlike PMVECs, PAECs only gave rise to relatively homogeneous slow-growing colonies. It is questionable whether single PAECs can reconstitute colonies of cells reflective of their parent population when they are

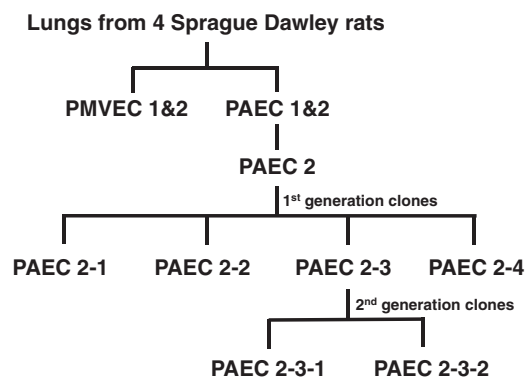


Fig. 3. Cell nomenclature is shown in the study design. PMVECs and PAECs were isolated from the lungs of four different male Sprague Dawley rats. PMVECs were isolated from two different rats (PMVEC 1 and 2), and PAECs were isolated from two separate rats (PAEC 1 and 2). PAEC 2 was single cell cloned to generate four randomly selected first-generation colonies, PAEC 2-1, 2-2, 2-3, and 2-4. PAEC 2-3 was single cell cloned to generate two second-generation colonies, PAEC 2-3-1 and 2-3-2.

expanded from single cell culture conditions. To answer this question, we randomly selected four colonies that were derived from single cell clones of PAEC 2 and named these first-generation clones PAEC 2-1, PAEC 2-2, PAEC 2-3, and PAEC 2-4 (Fig. 3). The population growth of these first-generation PAEC 2 clonal cells was almost identical to their parent cells, or slower in the case of PAEC 2-4 (Fig. 4a). There was no obvious medium color change by day 7 in any of the clones, indicating cells did not use aerobic glycolysis to sustain their growth. Notably, morphology of these cells was extremely homogeneous compared to their parent population. In subsequent single cell cloning experiments using the first-generation clones, only PAEC 2-3 grew detectable cell colonies, in 13 out of 384 wells of 96-well plates (Fig. 4b). The remaining wells possessed single cells, or small cell colonies not immediately detectable. PAEC 2-1, 2-2, and 2-4 did not grow detectable colonies within 14 days of cell seeding.

Matrigel assays revealed network formation in all first-generation clones. Cell seeding at 8.0×10^4 cells per well was necessary to observe network formation, which is identical to the seeding density of the parent cells (Fig. 4c). This seeding density is twofold higher than the typical seeding density for PMVECs. Network morphology of the cloned cells was similar to that seen in the parent cell populations, with thin webs and large luminal areas.

Mitochondrial and glycolysis stress tests revealed no significant difference among first-generation clones (Fig. 4d). Compared to the parent cells, all clones showed lower OCR at baseline (OCR at 0 min point in PAEC 2 vs. 2-1, vs. 2-2, vs. 2-3, and vs. 2-4, $P < 0.05$), whereas there was no difference in ECAR among the cells tested (Fig. 4d). Additional parameters for mitochondrial function, basal OCR, ATP-linked respiration, maximal respiration, and spare capacity were all similar among all clones except the differences

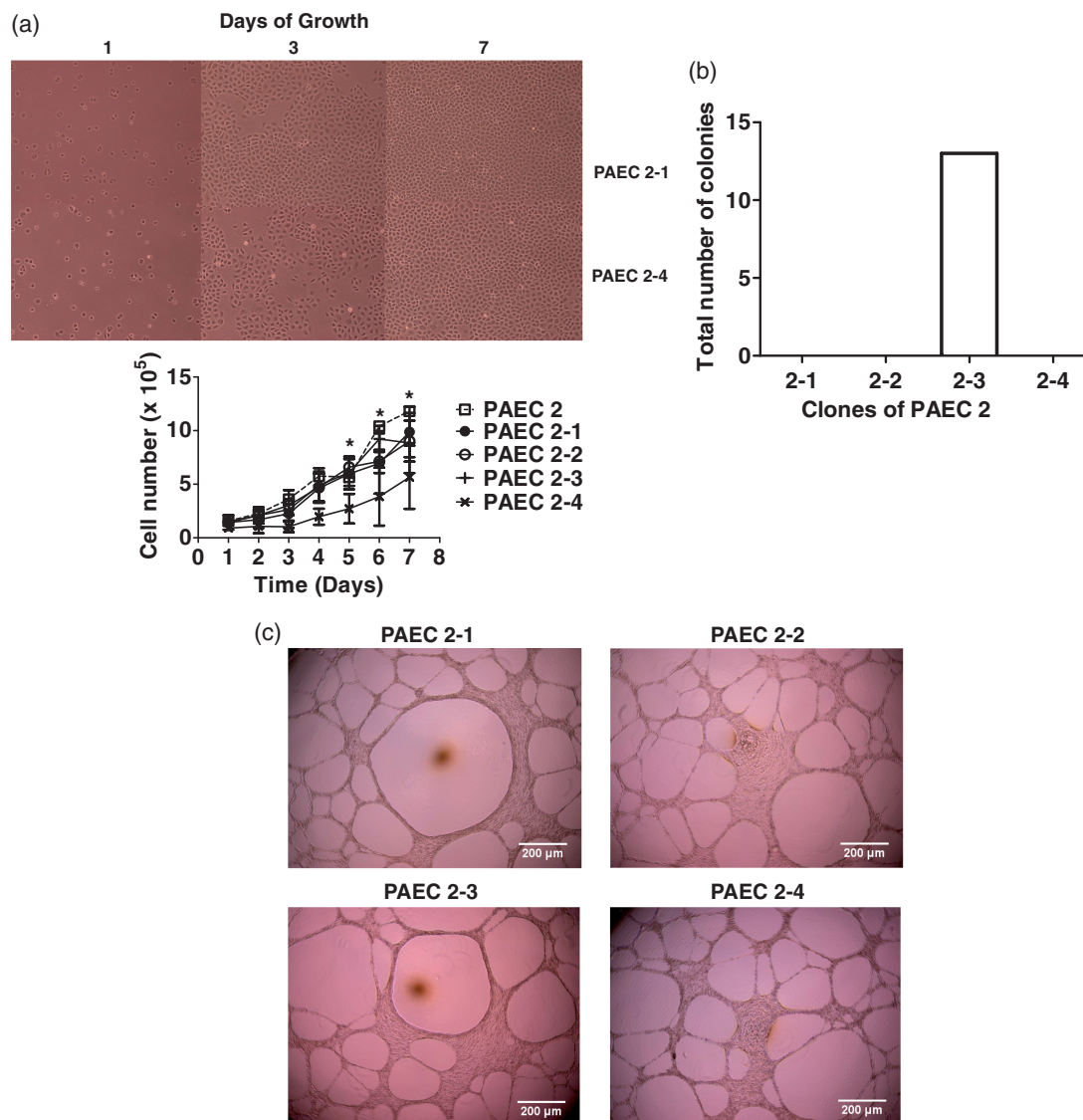


Fig. 4. First generation PAEC 2 clones closely mimic their parent population. (a) Serum stimulated growth of four first-generation clones of PAEC 2 were assessed. PAEC 2-1, 2-2, and 2-3 grew at a similar growth rate as their parent population. PAEC 2-4 showed decreased growth rate compared to the other clones. Data represent mean \pm standard deviation. Two-way ANOVA and Bonferroni post hoc tests were used to compare between cell types. For each cell type, two separate experiments were performed using a total of four wells. The PAEC 2 growth curve is depicted as a dotted line for a reference. *denotes significantly different ($P < 0.05$; PAEC 2-4 vs. PAEC 2-1, 2-2, or 2-3). Data were gathered from two independent experiments with four wells per group. PAEC 2 mean cell number values from Fig. 1a are depicted in a broken line for a reference. (b) PAEC 2-1, 2-2, 2-3 and 2-4 were seeded one cell per well on 96-well plates, four plates per cell type, by FACS sorting. Plates were examined on day 14. Only PAEC 2-3 had visible small-sized colonies, whereas PAEC 2-1, 2-2, and 2-4 did not grow discernible colonies. Data represent a total number of colonies in four plates. (c) PAEC 2 first generation clones were seeded on Matrigel coated 96-well plates at 8.0×10^4 cells per well. Images were obtained 24 h after seeding at $10 \times$ magnification. All first-generation PAEC 2 clones formed networks similar to their parent population. (d–f) The principal bioenergetic pathways utilized by PAEC 2 first-generation clones were determined by mitochondrial (d, e) and glycolysis (f) stress tests using the Seahorse extracellular flux analyzer. OCR and ECAR at baseline and with different mitochondrial (oligomycin, FCCP, and rotenone) and glycolytic (glucose, oligomycin, and 2-DG) stressors are shown over time. There was no significant difference between groups. Data represent mean \pm standard error. (d, f) Two-way ANOVA and Bonferroni post hoc test were used to compare between cell types. Results from three independent experiments, each with five replicates, a total of 15 wells per group are shown. Mean values of OCR and ECAR of PAEC 2 from Fig. 2a and d are depicted in broken lines for references. For the purposes of clarity standard deviation has been removed. *denotes significant difference ($P < 0.05$) PAEC 2 vs. 2-1, 2-2, 2-3, or 2-4 ($n = 3$ per group). (e) Basal OCR, ATP-linked respiration (average basal OCR – oligomycin response), maximal respiration (FCCP response), and spare capacity (maximal OCR – average basal OCR) are noted. One-way ANOVA and Bonferroni post hoc test were used to compare between cell types. Each dot represents the value of individual well at each time point. *denotes significant difference between PAEC 2-1 vs. 2-4. ^denotes significant difference between PAEC 2-2 vs. 2-4.

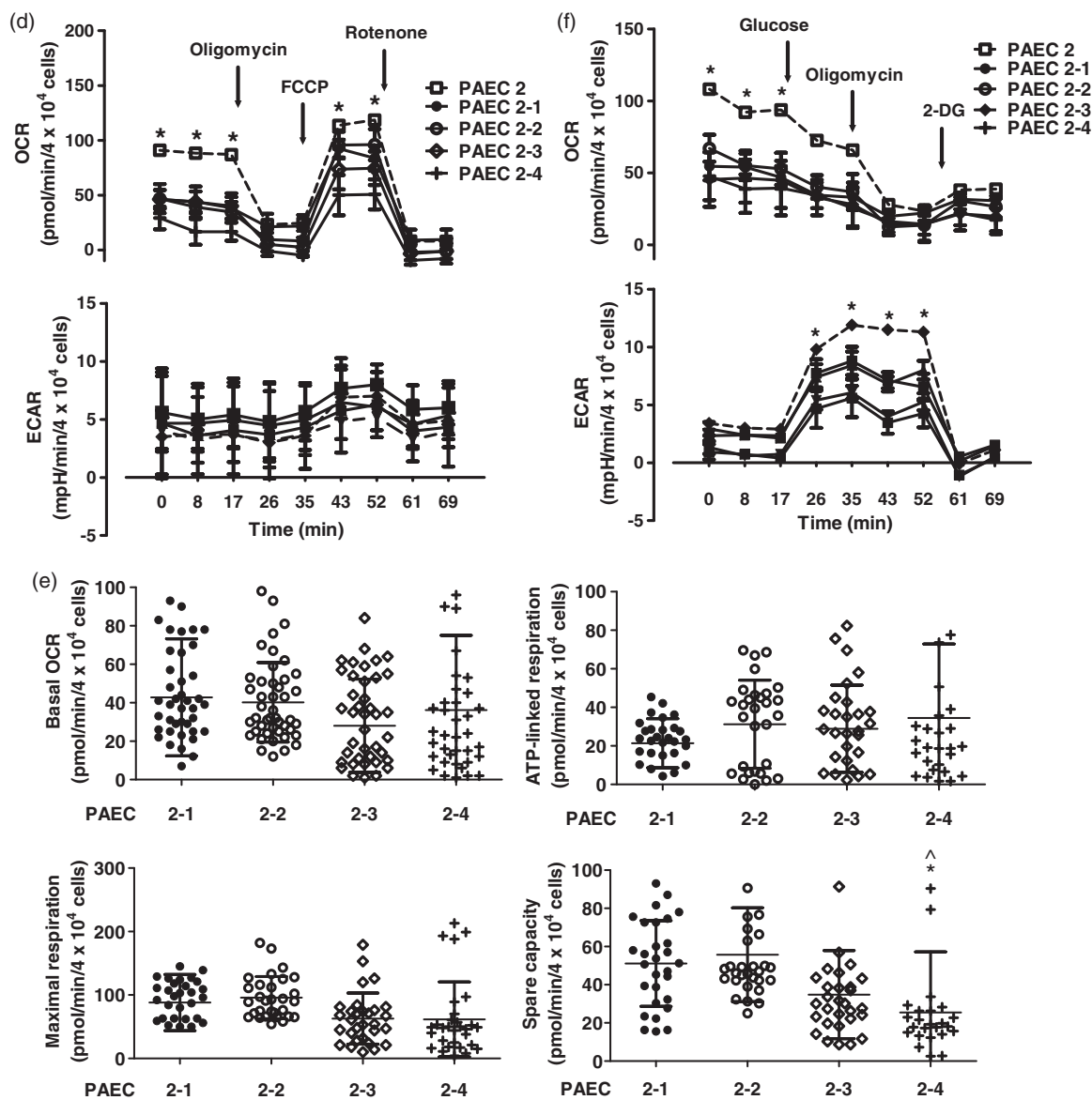


Fig. 4. Continued.

between PAEC 2- and other clones in spare capacity (Fig. 4e). During the glycolysis stress test, baseline OCR (OCR at 0 min in PAEC 2 vs. 2-1, vs. 2-2, vs. 2-3, and vs. 2-4, $P < 0.05$) and glucose challenged maximal ECAR (ECAR at 52 min in PAEC 2 vs. 2-1, vs. 2-2, vs. 2-3, and vs. 2-4, $P < 0.05$) were both reduced in the clones compared to the parent cells (Fig. 4f). Thus, whereas growth and angiogenic potential were nearly identical between the parental cells and the clonal derivatives, metabolic profiling indicated the first-generation PAEC clones had lower bioenergetic demands.

Second generation single cell cloning may select cells with relatively higher replication. PAEC populations that are initially isolated and expanded arise from within an arterial segment, but the expanded progeny are likely to derive

from multiple different cells within the vessel wall. For this reason, first-generation PAEC 2 clones may not necessarily be derived from the same cells. Therefore, we repeated single cell cloning on first-generation colonies to generate second-generation colonies (Fig. 3). These second-generation colonies are truly single cell progeny. Since PAEC 2-3 was the only first-generation clone that grew discernable colonies on single cell clonogenic assays, we randomly selected two colonies from the PAEC 2-3 single cell cloned plates, and named them PAEC 2-3-1 and PAEC 2-3-2.

PAEC 2-3-1 and 2-3-2 population growth was nearly identical, and was similar to their parent cells, PAEC 2-3 (Fig. 5a). However, in single cell studies, PAEC 2-3-1 and 2-3-2 revealed an increased number of colonies derived from single cells when compared to PAEC 2-3 (PAEC 2-3 vs.

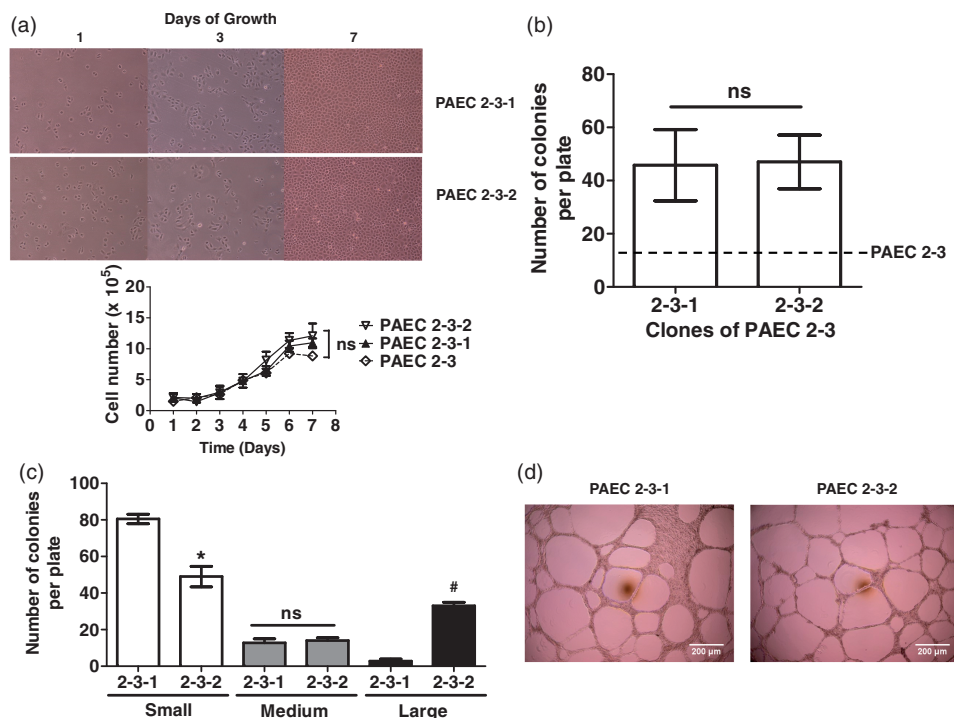


Fig. 5. Second-generation PAEC 2 clones mimic the parent population and possess increased replication competence. (a) Serum stimulated growth of two PAEC 2-3 second-generation clones were assessed. There was no significant difference between groups when compared to the parent population. Data represent mean \pm standard deviation. Two-way ANOVA and Bonferroni post hoc test were used to compare between cell types. ns denotes not significant. PAEC 2-3 growth curves are depicted as a dotted line for a reference. PAEC 2-2 mean values of cell number from Fig. 2a are depicted in a broken line for a reference. (b, c) PAEC 2-3-1 and 2-3-2 were seeded one cell per well on 96-well plates, four plates per cell type, by FACS sorting. (b) Plates were examined on day 14. There was no significant difference between groups in total numbers of colony counts. The absolute colony counts are increased in both PAEC 2-3-1 and 2-3-2 compared to PAEC 2-3. Data represent number of colonies per plate, mean \pm standard deviation. Unpaired *t*-test was used to compare between two groups. ns, not significant. A total number of colonies observed in single cell clonogenic assays of PAEC 2-3 is depicted in a broken line for a reference. (c) Plates were reexamined on day 28. Over this extended time course, both second-generation PAEC 2 clones reconstituted a hierarchy of small- to large-sized colonies. PAEC 2-3-1 had a lower number of large-sized colonies than PAEC 2-3-2. *denotes significantly different ($P < 0.05$) compared to PAEC 2-3-1 vs. 2-3-2 in small-sized colonies. ns, not significant. # denotes significantly different ($P < 0.05$) compared to PAEC 2-3-1 vs. PAEC 2-3-2 in large-sized colonies. (d) Cells were seeded on Matrigel (30 μ L per well) coated 96-well plates at densities of 8.0×10^4 cells depending on a cell type at a total cell solution volume of 80 μ L. Cells were incubated at 37 $^{\circ}$ C with 5% CO₂-room air for 24 h and then observed and pictures taken. Images are at 10 \times magnification. Both PAEC 2-3-1 and 2-3-2 formed thin networks with large luminal areas similar to those of PAEC 2 and 2-3. (e–h) The principal bioenergetic pathways utilized by PAEC 2-3-1 and 2-3-2 were determined by mitochondrial (e–g) and glycolysis (h) stress tests using the Seahorse extracellular flux analyzer. OCR and ECAR at baseline and with different mitochondrial (oligomycin, FCCP, and rotenone) and glycolytic (glucose, oligomycin, and 2-DG) stressors are shown over time. PAEC 2-3-1 showed decreased aerobic glycolysis and increased oxidative phosphorylation when compared to PAEC 2-3-2. OCR and ECAR patterns of 2-3-2 closely mimicked those of PAEC 2-3. Data represent mean \pm standard error. Two-way ANOVA and Bonferroni post hoc test were used to compare between cell types. Results from three independent experiments, each with five replicates, a total of 15 wells per group are shown. *denotes significantly different ($P < 0.05$) in PAEC 2-3-1 vs. PAEC 2-3-2 ($n = 3$ per group). Mean values of OCR and ECAR of PAEC 2-3 from Fig. 4d and f are depicted in broken lines for references. For the purposes of clarity standard deviation has been removed. (f) Basal OCR, ATP-linked respiration (average basal OCR – oligomycin response), maximal respiration (FCCP response), and spare capacity (maximal OCR – average basal OCR) are noted. (g) ECAR at baseline of mitochondrial stress test at three different time points are depicted. Each dot represents the value of individual well at each time point. Student's *t*-test was used. *denotes significant difference ($P < 0.05$) between PAEC 2-3-1 vs. 2-3-2.

2-3-1 vs. 2-3-2, $P < 0.05$); there was no difference in the single cell growth potential among PAEC 2-3-1 and 2-3-2 (Fig. 5b; $P = ns$). Thus, in this experiment, the growth of single cell clones did not broadly reflect the population growth curves.

We considered this potential paradox further. Here, single cell studies were repeated, and the growth period

extended from 14 days to 28 days after the initial cell seeding (Fig. 5c). On longer observation, PAEC clones grew to variable colony sizes, just as shown in PMVECs (Fig. 1b).^{8,26} The time required to develop the growth hierarchy was longer and the number of high proliferative potential colonies was lower than previously observed in PMVECs.^{8,26} Comparing between the two different second-generation

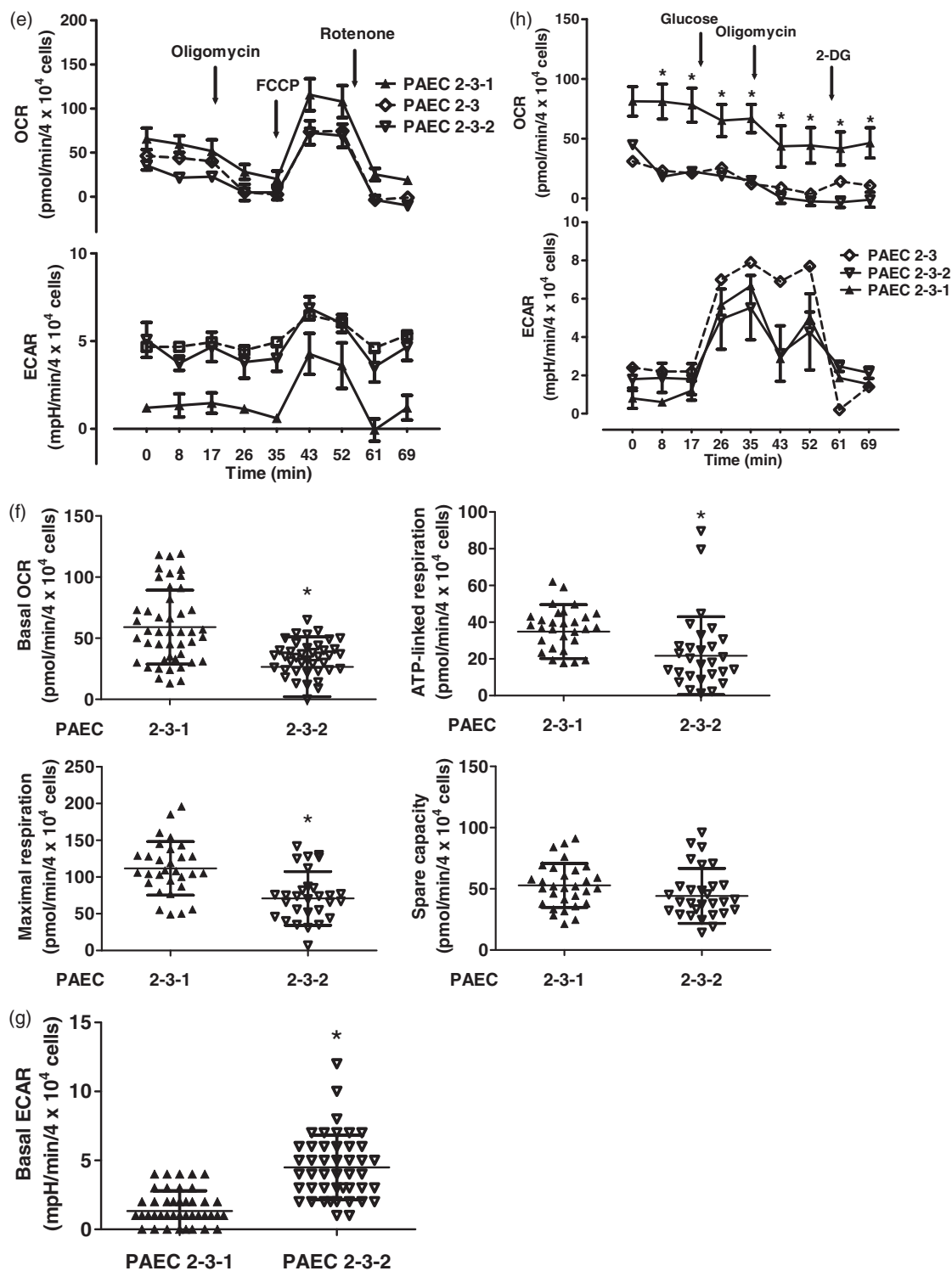


Fig. 5. Continued.

clones, PAEC 2-3-1 had a significantly lower number of large colonies than PAEC 2-3-2 (PAEC 2-3-1 vs. 2-3-2, $P < 0.05$). None of the PAEC 2-3-1 clones acidified the medium, whereas several PAEC 2-3-2 clones displayed aerobic glycolysis.

Matrigel assay findings corroborated the growth curve results, as network formation was identical in PAEC 2-3-1 and 2-3-2 (Fig. 5d). The number of cells required to form stable networks was identical to that of their parent cells, which was 8.0×10^4 cells per well. The pattern of network

formation, including thin webs and large lumens, was similar to that of their parent cells as well.

Although there was no significant difference between PAEC 2-3-1 and PAEC 2-3-2 in population growth and Matrigel network patterns, single cell proliferative capacity was lower in PAEC 2-3-1. Consistent with this decrease in single cell proliferative potential difference, mitochondrial and glycolysis stress tests revealed significantly decreased aerobic glycolysis utilization in PAEC 2-3-1 compared to PAEC 2-3-2 (Fig. 5e–h). In the mitochondrial stress test, OCR was higher (PAEC 2-3-1 vs. 2-3-2, $P < 0.05$) and ECAR was lower (PAEC 2-3-1 vs. 2-3-2, $P < 0.05$) at baseline in PAEC 2-3-1, suggesting higher oxidative phosphorylation and less dependence on aerobic glycolysis (Fig. 5e–g). Additional parameters for mitochondrial function, basal OCR, ATP-linked respiration, and maximal respiration were all higher (PAEC 2-3-1 vs. 2-3-2, $P < 0.05$) in PAEC 2-3-1 (Fig. 5f). Consistent findings were observed in the glycolysis stress test, where OCR was higher in PAEC 2-3-1 (PAEC 2-3-1 vs. 2-3-2, $P < 0.05$) and ECAR was relatively suppressed in PAEC 2-3-1 at baseline (PAEC 2-3-1 vs. 2-3-2, $P = ns$) (Fig. 5h). Overall, the metabolic profile of PAEC 2-3-2 was nearly identical to the parental cell line, PAEC 2-3.

Discussion

Pulmonary endothelial cells are structurally and functionally heterogeneous.^{8,26} They possess differential characteristics in population growth, single cell cloning, angiogenesis, and bioenergetic pathway utilization. In this study, we have examined PMVECs and PAECs isolated from multiple rats to rigorously test generalizability of our previous findings. Then, we cloned PAECs and compared them to the parent cells to evaluate how well clones represent parental characteristics. We studied PAECs because they possess fewer high proliferative potential cells within the population. The results recapitulated and expanded previously identified typical characteristics of PMVECs and PAECs. Using cells from different animals, PMVECs grew faster in population and had a higher proliferative potential in single cell cloning than PAECs, they required fewer cells to form networks in Matrigel compared to PAECs, and they were more reliant upon aerobic glycolysis. First-generation clones of selected PAECs were highly representative of the parental population. Second-generation clones of selected PAECs had enhanced replication competence in single cell conditions, but maintained parental characteristics. They were also noted to be morphologically homogeneous within each clonal population, making sibling clones more distinctive from each other.

Replication competence is a critical feature of the cells used in in vitro studies. However, repeated subculture increases the risk for phenotypic drift.³⁰ Although such phenotypic drift has been reported in cell types such as cancer cell lines³¹ and mesenchymal stem cells,³² and discussions regarding environmental influences of endothelial cell

phenotype is widespread, it is not known how typical characteristics of PMVECs and PAECs, including growth, angiogenic potential, and bioenergetic demands, are affected by repeated subculture. Furthermore, little is known regarding how single cell cloning and expansion alters these endothelial cell properties, given that each cell in the single cell assay starts growing in the absence of signals from neighboring cells. We have evaluated characteristics of two consecutive clonal generations from one PAEC parental population. PAECs are isolated from the main pulmonary trunk and one to two vascular bifurcations. Therefore, cells within a cultured population could be diverse, having originated in either the same or different pulmonary artery region (Fig. 6). As a result, isolation of first-generation clones separates these diverse parental populations from each other. In contrast, second-generation clones are truly derived from a single cell. Interestingly, as clonal generation increased, there was a clear increase in the single cell replication competence. However, their population growth, angiogenic potential, and bioenergetic characteristics remained relatively unchanged. Furthermore, second-generation clones seemed to be more homogeneous within each clonal population. Second-generation clones also remained similar to their parental cells, PAECs, relative to PMVECs. Therefore, our data suggest that single cell cloning could be utilized to expand a small number of cells while preserving parental characteristics. It also can potentially be used to choose clonal populations that have higher replication competence in single cell conditions, while possessing more homogeneous characteristics of parental cells.

The bioenergetic demands of endothelial cell function, including maintenance of a semi-permeable barrier, angiogenesis, and control of vascular tone, require significant ATP production.¹ However, Oldendorf et al. estimated mitochondrial endothelial cell volume is only 2–5% of the total cytoplasmic volume in non-blood brain barrier capillaries,³³ a significantly lower volume compared to cardiac myocytes, which is 22–37%,³⁴ consistent with use of glycolysis rather than aerobic respiration to maintain ATP concentrations. Mertens et al. demonstrated that in the presence of glucose, endothelial respiration was independent of the exterior $PO_2 > 3$ Torr, and oxygen consumption was half maximal only under extreme hypoxia of 0.8 Torr of PO_2 .³⁵ Subsequent studies have shown that endothelial cell metabolism closely mimics that of cancer cells, primarily utilizing aerobic glycolysis to produce ATP.³⁶ In comparing baseline glycolysis among endothelial cells, selected cancer cells, and cells such as neurons, hepatocytes, and cardiomyocytes,³⁷ endothelial cell glycolytic flux was similar to cancer cells and significantly higher than the other healthy cells. Oxygen consumption rates were consistently lower in endothelial cells compared to neurons, hepatocytes, and cardiomyocytes. Endothelial cell glycolytic flux was >200-fold higher than glucose, fatty acid, and glutamine oxidation, and ATP generated by glycolysis approached 85% of the total cellular ATP content. The largest energy yield was

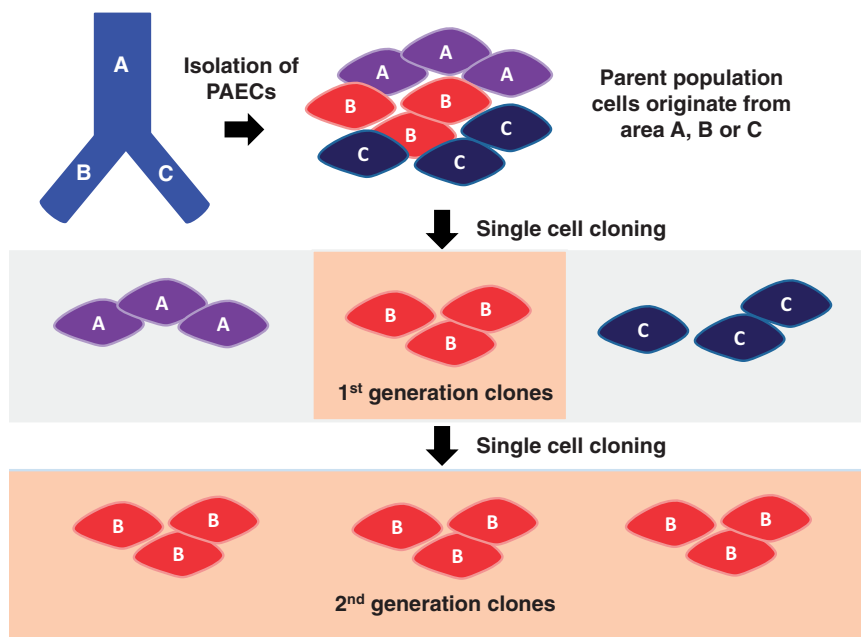


Fig. 6. Second-generation single cell clones arise from one cell phenotype. Cells within the parental population may originate from different areas within the pulmonary artery (e.g. A, B and/or C areas). By single cell cloning, first-generation clones are generated, which separate potentially heterogeneous cells from one another. Repeated single cell cloning generates second-generation clones; these clones arise from one cell phenotype. Tan shaded regions of “B” cells represent clones isolated from the first and second cloning strategies, respectively.

obtained by glycolytic breakdown of glucose compared to palmitate, lactate, and glutamine in coronary microvascular endothelial cells.³⁸ Ninety-nine percent of glucose was degraded to lactate and only 0.04% was oxidized in the Krebs cycle. One percent was catabolized via the hexose monophosphate pathway. These data suggest aerobic glycolysis is a primary mechanism of ATP production in endothelial cells. This highly glycolytic property has been described in endothelial cells of different vascular origin (Table 1).

Our present study shows that both PMVECs and PAECs utilize aerobic glycolysis. Although PAECs have lower rates of aerobic glycolysis at baseline, they are still able to mount significant ECAR with relatively suppressed OCR upon glucose loading. This phenomenon of increased aerobic glycolysis and repressed oxidative phosphorylation in the setting of increased glucose availability is defined by the Crabtree effect,³⁹ which is commonly observed in rapidly growing cancer cells along with the Warburg effect. However, the degree of dependence on aerobic glycolysis is significantly different between PMVECs and PAECs at baseline. It is not yet clear whether these findings directly represent the PMVEC and PAEC phenotype in vivo.

The reason endothelial cells utilize aerobic glycolysis is incompletely understood. It may be that they gain an advantage from utilizing aerobic glycolysis, or it may be that they are driven to use aerobic glycolysis due to relative impairment in mitochondrial function. Carmiliet et al. hypothesized that endothelial cells prefer utilizing aerobic

glycolysis for multiple reasons, including decreased oxygen consumption and reactive oxygen species production, which confers a survival advantage and enables development of new vascular structures in oxygen deprived environments.³⁶ Furthermore, aerobic glycolysis is a faster way of producing ATP than is oxidative phosphorylation when there is a sufficient glucose supply and simultaneous activation of macromolecule producing pathways that provide biomass for rapidly proliferating cells. These advantages of aerobic glycolysis may be most useful for capillary endothelial cells that are responsible for the gas exchange barrier, whereas arterial endothelial cells contribute to vascular tone for blood delivery to the capillaries. Relative impairment in mitochondrial function was hypothesized given that some cancer cells are known to utilize aerobic glycolysis due to increased pyruvate dehydrogenase kinase (PDK) expression, which inhibits oxidative phosphorylation.^{40–42} However, RNA sequencing of PMVECs and PAECs revealed no significant difference in PDK1-4 expression between two cell types.

In summary, we report distinctive proliferation, network forming (e.g. angiogenesis) and bioenergetic capacities of PMVECs and PAECs, which are preserved in multiple clonal generations in PAECs. These findings offer an approach to generate replication competent progeny for in vitro experiments and shed novel insight into the preservation of single cell inheritance. Indeed, these findings continue to support the idea that macrovascular and microvascular cell lineages retain certain memories of their origins under culture conditions.

Table 1. Review of studies on aerobic glycolysis in endothelial cells.

Type of cells	Key findings	Reference
Rat PMVECs and PAECs	PMVECs utilize aerobic glycolysis whereas PAECs utilize oxidative phosphorylation as primary energy yielding pathway	8
Human PAECs	PAECs isolated from idiopathic pulmonary arterial hypertension patients exhibit increased aerobic glycolysis	43
Human PMVECs	Isocitrate dehydrogenase activity is increased in hPMVEC expressing mutant BMPR2 and in the serum of pulmonary arterial hypertension patients	44
	2-DG inhibited endothelial cell angiogenesis <i>in vitro</i> and <i>in vivo</i>	45
Human umbilical vein endothelial cells	Endothelial cells rely on glycolysis and loss of the glycolytic activator 6-phosphofructo-2-kinase/Fructose-2,6-Biphosphatase 3 (PFKFB3) impaired vessel formation	37
	ATP production was moderately decreased (30%) by mitochondrial inhibitors or low oxygen concentration of < 0.5%. However, inhibition of glycolysis pathway was more potent to decrease ATP production to a higher degree of >50%	46
	HUVEC showed a high glycolytic and NADPH regenerating capacity	47
	2-DG inhibited endothelial cell angiogenesis <i>in vitro</i> and <i>in vivo</i>	45
Bovine aortic endothelial cells	Treatment of BAEC with 2-DG (5 mM) for 24 h induced autophagy	48
	Measured by extracellular flux analysis, endothelial cells use only approximately 35% of their maximal respiratory capacity.	49
Pig aortic endothelial cells	Measured by calorimetry and ³¹ P nuclear magnetic resonance, at least three-fourths of ATP synthesized was shown to be provided by glycolysis in endothelial cells. They also exhibit the ability to downregulate ATP synthesis and consumption when glycolysis is inhibited	50
Rat coronary endothelial cells	In saline medium containing 5 mM glucose, 99.3% of all glucose catabolized was degraded to lactate measured by (U- ¹⁴ C) labelled L-lactate. Only 6% of CO ₂ produced by glucose degradation originated from the Krebs cycle	51
Rat liver endothelial cells	Endothelial cells have significantly lower mitochondrial volume compared to that of hepatocyte (4.26 ± 0.39% vs. 28.32 ± 0.50%).	52

Acknowledgements

The authors thank Drs. Mikhail Alexeyev, Ming Tan, and Sangbin Lim and Ms. Natalya Kozhukhar for their assistance with Seahorse assays and Dr. Domenico Spadafora for single cell clonogenic assays.

Conflict of interest

The author(s) declare that there is no conflict of interest.

Funding

This research was supported by HL66299 (TS), HL60024 (TS), and HL117721 (SAM).

References

- Aird WC. Endothelial cell heterogeneity. *Cold Spring Harb Perspect Med* 2012; 2: a006429.
- Fuchs A and Weibel ER. Morphometrische untersuchung der verteilung einer spezifischen cytoplasmatischen organelle in endothelzellen der ratte. *Zeitschrift für Zellforschung und Mikroskopische Anatomie* 1966; 73: 1–9.
- Steinsiepe KF and Weibel ER. Electron microscopic studies on specific organelles of endothelial cells in the frog (*Rana temporaria*). *Zeitschrift für Zellforschung und Mikroskopische Anatomie* 1970; 108: 105–126.
- Weibel ER. Fifty years of Weibel-Palade bodies: the discovery and early history of an enigmatic organelle of endothelial cells. *J Thromb Haemost* 2012; 10: 979–984.
- Kelly JJ, Moore TM, Babal P, et al. Pulmonary microvascular and macrovascular endothelial cells: differential regulation of Ca²⁺ and permeability. *Am J Physiol* 1998; 274: L810–L819.
- King J, Hamil T, Creighton J, et al. Structural and functional characteristics of lung macro- and microvascular endothelial cell phenotypes. *Microvasc Res* 2004; 67: 139–151.
- Moore TM, Brough GH, Babal P, et al. Store-operated calcium entry promotes shape change in pulmonary endothelial cells expressing Trp1. *Am J Physiol* 1998; 275: L574–L582.
- Parra-Bonilla G, Alvarez DF, Al-Mehdi AB, et al. Critical role for lactate dehydrogenase A in aerobic glycolysis that sustains pulmonary microvascular endothelial cell proliferation. *Am J Physiol Lung Cell Mol Physiol* 2010; 299: L513–522.
- Cioffi DL, Lowe K, Alvarez DF, et al. TRP on the lung endothelium: calcium channels that regulate barrier function. *Antioxid Redox Signal* 2009; 11: 765–776.
- Cioffi DL and Stevens T. Regulation of endothelial cell barrier function by store-operated calcium entry. *Microcirculation* 2006; 13: 709–723.
- Cioffi DL, Wu S and Stevens T. On the endothelial cell I SOC. *Cell Calcium* 2003; 33: 323–336.
- Cioffi DL, Pandey S, Alvarez DF, et al. Terminal sialic acids are an important determinant of pulmonary endothelial

- barrier integrity. *Am J Physiol Lung Cell Mol Physiol* 2012; 302: L1067–L1077.
13. Scarritt ME, Pashos NC, Motherwell JM, et al. Re-endothelialization of rat lung scaffolds through passive, gravity-driven seeding of segment-specific pulmonary endothelial cells. *J Tissue Eng Regen Med* 2016; doi: 10.1002/term.2382.
 14. Gebb S and Stevens T. On lung endothelial cell heterogeneity. *Microvasc Res* 2004; 68: 1–12.
 15. Ochoa CD and Stevens T. Studies on the cell biology of inter-endothelial cell gaps. *Am J Physiol Lung Cell Mol Physiol* 2012; 302: L275–286.
 16. Ochoa CD, Wu S and Stevens T. New developments in lung endothelial heterogeneity: Von Willebrand factor, P-selectin, and the Weibel-Palade body. *Semin Thromb Hemost* 2010; 36: 301–308.
 17. Stevens T. Molecular and cellular determinants of lung endothelial cell heterogeneity. *Chest* 2005; 128: 558s–564s.
 18. Majno G and Palade G. Studies on inflammation: I. The effect of histamine and serotonin on vascular permeability: An electron microscopic study. *J Biophys Biochem Cytol* 1961; 11: 571.
 19. Francis M, Xu N, Zhou C, et al. Transient receptor potential channel 4 encodes a vascular permeability defect and high-frequency Ca(2+) transients in severe pulmonary arterial hypertension. *Am J Pathol* 2016; 186: 1701–1709.
 20. Taylor MS, Choi CS, Bayazid L, et al. Changes in vascular reactivity and endothelial Ca²⁺ dynamics with chronic low flow. *Microcirculation* 2017; 24: e12354.
 21. Schwartz SM and Benditt EP. Clustering of replicating cells in aortic endothelium. *Proc Natl Acad Sci U S A* 1976; 73: 651–653.
 22. Ingram DA, Mead LE, Moore DB, et al. Vessel wall-derived endothelial cells rapidly proliferate because they contain a complete hierarchy of endothelial progenitor cells. *Blood* 2005; 105: 2783–2786.
 23. Ingram DA, Mead LE, Tanaka H, et al. Identification of a novel hierarchy of endothelial progenitor cells using human peripheral and umbilical cord blood. *Blood* 2004; 104: 2752–2760.
 24. Yoder MC, Mead LE, Prater D, et al. Redefining endothelial progenitor cells via clonal analysis and hematopoietic stem/progenitor cell principals. *Blood* 2007; 109: 1801–1809.
 25. Sims-Lucas S, Schaefer C, Bushnell D, et al. Endothelial progenitors exist within the kidney and lung mesenchyme. *PLoS One* 2013; 8: e65993.
 26. Alvarez DF, Huang L, King JA, et al. Lung microvascular endothelium is enriched with progenitor cells that exhibit vasculogenic capacity. *Am J Physiol Lung Cell Mol Physiol* 2008; 294: L419–L430.
 27. Creighton JR, Masada N, Cooper DM, et al. Coordinate regulation of membrane cAMP by Ca²⁺-inhibited adenylyl cyclase and phosphodiesterase activities. *Am J Physiol Lung Cell Mol Physiol* 2003; 284: L100–107.
 28. Stevens T, Creighton J and Thompson WJ. Control of cAMP in lung endothelial cell phenotypes. Implications for control of barrier function. *Am J Physiol* 1999; 277: L119–126.
 29. Ingram DA, Caplice NM and Yoder MC. Unresolved questions, changing definitions, and novel paradigms for defining endothelial progenitor cells. *Blood* 2005; 106: 1525–1531.
 30. Geraghty RJ, Capes-Davis A, Davis JM, et al. Guidelines for the use of cell lines in biomedical research. *Br J Cancer* 2014; 111: 1021–1046.
 31. Torsvik A, Stieber D, Enger PØ, et al. U-251 revisited: genetic drift and phenotypic consequences of long-term cultures of glioblastoma cells. *Cancer Med* 2014; 3: 812–824.
 32. Binato R, de Souza Fernandez T, Lazzarotto-Silva C, et al. Stability of human mesenchymal stem cells during in vitro culture: considerations for cell therapy. *Cell Prolif* 2013; 46: 10–22.
 33. Oldendorf WH, Cornford ME and Brown WJ. The large apparent work capability of the blood-brain barrier: A study of the mitochondrial content of capillary endothelial cells in brain and other tissues of the rat. *Ann Neurol* 1977; 1: 409–417.
 34. Barth E, Stämmler G, Speiser B, et al. Ultrastructural quantitation of mitochondria and myofilaments in cardiac muscle from 10 different animal species including man. *J Mol Cell Cardiol* 1992; 24: 669–681.
 35. Mertens S, Noll T, Spahr R, et al. Energetic response of coronary endothelial cells to hypoxia. *Am J Physiol* 1990; 258: H689–694.
 36. Verdegem D, Moens S, Stapor P, et al. Endothelial cell metabolism: parallels and divergences with cancer cell metabolism. *Cancer Metab* 2014; 2: 19.
 37. De Bock K, Georgiadou M, Schoors S, et al. Role of PFKFB3-driven glycolysis in vessel sprouting. *Cell* 2013; 154: 651–663.
 38. Spahr R, Krutzfeldt A, Mertens S, et al. Fatty acids are not an important fuel for coronary microvascular endothelial cells. *Mol Cell Biochem* 1989; 88: 59–64.
 39. Crabtree HG. The carbohydrate metabolism of certain pathological overgrowths. *Biochem J* 1928; 22: 1289–1298.
 40. Kamarajugadda S, Stemborski L, Cai Q, et al. Glucose oxidation modulates anoikis and tumor metastasis. *Mol Cell Biol* 2012; 32: 1893–1907.
 41. Lu C-W, Lin S-C, Chien C-W, et al. Overexpression of pyruvate dehydrogenase kinase 3 increases drug resistance and early recurrence in colon cancer. *Am J Pathol* 2011; 179: 1405–1414.
 42. Shen YC, Ou DL, Hsu C, et al. Activating oxidative phosphorylation by a pyruvate dehydrogenase kinase inhibitor overcomes sorafenib resistance of hepatocellular carcinoma. *Br J Cancer* 2013; 108: 72–81.
 43. Xu W, Koeck T, Lara AR, et al. Alterations of cellular bioenergetics in pulmonary artery endothelial cells. *Proc Natl Acad Sci* 2007; 104: 1342–1347.
 44. Fessel JP, Hamid R, Wittmann BM, et al. Metabolomic analysis of bone morphogenetic protein receptor type 2 mutations in human pulmonary endothelium reveals widespread metabolic reprogramming. *Pulm Circ* 2012; 2: 201–213.
 45. Merchan JR, Kovács K, Railsback JW, et al. Antiangiogenic activity of 2-deoxy-D-glucose. *PLoS One* 2010; 5: e13699.
 46. Quintero M, Colombo SL, Godfrey A, et al. Mitochondria as signaling organelles in the vascular endothelium. *Proc Natl Acad Sci U S A* 2006; 103: 5379–5384.
 47. Peters K, Kamp G, Berz A, et al. Changes in human endothelial cell energy metabolic capacities during in vitro cultivation. The role of “aerobic glycolysis” and proliferation. *Cell Physiol Biochem* 2009; 24: 483–492.
 48. Wang Q, Liang B, Shirwany NA, et al. 2-Deoxy-D-glucose treatment of endothelial cells induces autophagy by reactive

- oxygen species-mediated activation of the AMP-activated protein kinase. *PLoS One* 2011; 6: e17234.
49. Dranka BP, Hill BG and Darley-USmar VM. Mitochondrial reserve capacity in endothelial cells: The impact of nitric oxide and reactive oxygen species. *Free Radic Biol Med* 2010; 48: 905–914.
 50. Culic OG, Gruwel ML and Schrader JU. Energy turnover of vascular endothelial cells. *Am J Physiol Cell Physiol* 1997; 273: C205–13.
 51. Krützfeldt A, Spahr R, Mertens S, et al. Metabolism of exogenous substrates by coronary endothelial cells in culture. *J Mol Cell Cardiol* 1990; 22: 1393–1404.
 52. Blouin A, Bolender RP and Weibel ER. Distribution of organelles and membranes between hepatocytes and nonhepatocytes in the rat liver parenchyma. A stereological study. *J Cell Biol* 1977; 72: 441–455.